ARCHIVIO ISTITUZIONALE
DELLA RICERCA

Alma Mater Studiorum Università di Bologna
Archivio istituzionale della ricerca

Improving the accuracy of vibration reduction index measurements: Assessing and correcting parasitic airborne noise effects

This is the final peer-reviewed author's accepted manuscript (postprint) of the following publication:

Published Version:
Crispin, C., Pettoni Possenti, V., Dijckmans, A., Barbaresi, L. (2025). Improving the accuracy of vibration reduction index measurements: Assessing and correcting parasitic airborne noise effects. APPLIED ACOUSTICS, 238, 1-11 [10.1016/j.apacoust.2025.110775].

Availability:
This version is available at: https://hdl.handle.net/11585/1016333 since: 2025-05-23

Published:

DOI: http://doi.org/10.1016/j.apacoust.2025.110775

Terms of use:

Some rights reserved. The terms and conditions for the reuse of this version of the manuscript are specified in the publishing policy. For all terms of use and more information see the publisher's website.

This item was downloaded from IRIS Università di Bologna (https://cris.unibo.it/).
When citing, please refer to the published version.

(Article begins on next page)

06 November 2026

Improving the Accuracy of Vibration Reduction Index Measurements: Assessing and Correcting Parasitic Airborne Noise Effects

Charlotte Crispin [a], Vincenzo Pettoni Possenti [b], Arne Dijckmans [a], Luca Barbaresi [b]

[a] *Buildwise, Kleine Kloosterstraat 23, B-1932 Zaventem, Belgium*

[b] *Department of Industrial Engineering, University of Bologna, Italy*

ABSTRACT

The vibration reduction index K_{ij}, measured in accordance with ISO 10848, is used to assess the attenuation of vibration transmissions at junctions between structural elements. In particular, it is used to compare the performance of different junctions or as input data for predictive calculations in the ISO 12354 standards series.

However, this measurement can be affected by parasitic airborne noise generated by the excitation source and acoustic radiation from the excited wall, leading to an underestimation of K_{ij}, particularly for high-performance junctions such as those incorporating resilient strips.

This article presents the results of numerical simulations based on the finite element method and experimental measurements carried out on two CLT mock-ups in two laboratories, one in Italy and the other in Belgium. These analyses highlight the influence of parasitic airborne noise on *Kij* measurements and underline the importance of minimising it as much as possible during testing to ensure the reliability of the values obtained. If this is not possible, a correction based on the subtraction of the contribution of unwanted airborne noise can be applied to improve the accuracy of the results.

The conclusions of this study are generalizable to any type of construction element and also to in situ measurements. The issue of incorporating parasitic airborne transmission into the predictive calculations of ISO 12354 standards is therefore raised, particularly when the construction elements of junctions incorporating a resilient strip are not combined with a lining or floating screed.

1. Introduction

With the increasing request for comfort inside buildings, sound insulation is becoming more and more critical. In order to have proper sound insulation in the building, in addition to direct sound transmission through walls, floors, and façades, secondary paths that propagate through the structure, flanking transmission, must also be considered.

The contribution of flanking transmission on the airborne sound insulation or on the impact sound insulation can be estimated following the ISO 12354 standard series [1] [2], which provides a simplified calculation method for predicting sound insulation between rooms. The model input parameters are the acoustic performance of construction elements and the

effectiveness of junctions in reducing structure-borne transmissions formalised by the vibration reduction index, K_{ij} or the normalized direction-average vibration level difference, $\overline{D_{v,ij,n}}$[3].

The vibration reduction index, K_{ij}, which represents the attenuation of vibratory power at the junction, is measured in the laboratory in accordance with the standard ISO 10848-1 [4]. One way of effectively reducing structural transmissions across a junction and therefore achieving a very high K_{ij} is to insert a resilient strip at the junction between a wall and a floor [5] [6] [7]. This technique, first studied by P. Mees [8], has been successfully applied to light masonry constructions [9] [10] [11] and is the subject of detailed applicability studies for cross-laminated timber (CLT) constructions [12] [13] [14] [15]. These studies require knowledge of the actual effectiveness of the resilient strips used at the junctions [16].

This article re-examines the measurement procedure of the vibration reduction index according to ISO 10848-1 for these high-insulated junctions and the problems when dealing with materials with a high radiation efficiency in the frequency range of interest, such as wood and cross-laminated timber (CLT) [17] where any vibration entering the panel is easily re-radiated by the entire panel surface [18] [19] [20] [21].

The vibration reduction index, measured according to ISO 10848, may be underestimated due to parasitic airborne noise generated by the excitation source and the acoustic radiation from the excited panel, particularly for high-performance junctions such as those with resilient strips. This article examines the impact of this parasitic airborne noise on the measurement of K_{ij} and on the predictive calculations of the ISO 12354 standard. To study this phenomenon, finite element method (FEM) numerical simulations were carried out, together with experimental measurements carried out in two specialised laboratories on high-insulation junctions, one in Italy and the other in Belgium.

2. The contribution of parasitic airborne noise transmission

The amount of vibration power transmitted by structural waves through a junction can be measured using the test procedure described in the ISO 10848 standards series. This quantity is obtained by measuring the direction-averaged velocity level difference $\overline{D_{v,ij}}$ between two connected building elements “i” and “j”:

$$\overline{D_{v,ij}} = \frac{D_{v,ij} + D_{v,ji}}{2} \qquad \text{[dB]} \tag{1}$$

in which $D_{v,ij}$ ($D_{v,ji}$) is the velocity level difference between source element *i* (element *j)* and receiver element *j* (element *i)*.

By normalizing this direction-averaged velocity level difference as a function of the length of the connection and the equivalent sound absorption length, you obtain the vibration reduction index K_{ij} as defined in the standard ISO 10848:

$$K_{ij} = \overline{D_{v,ij}} + 10\lg\left(\frac{L_{ij}}{\sqrt{a_i a_j}}\right) \text{ [dB]} \tag{2}$$

where L_{ij} is the junction length between elements i and j, and a_i and a_j are the equivalent absorption lengths of elements i and j, respectively.

However, during a test, the airborne noise generated by the impact of the excitation source and by the acoustic radiation from the excited wall can also induce vibrations on the receiving wall, thus affecting the K_{ij} measurement (fig.1). It is therefore essential not to neglect this contribution when measuring K_{ij}, particularly for junctions offering high attenuation of structural transmission, such as those incorporating a resilient strip.

During laboratory K_{ij} tests, whether to assess the effectiveness of resilient strips or to provide input data for the predictive models in the ISO 12354 standards series, the influence of airborne noise must be taken into account. If it proves impossible to eliminate parasitic airborne noise during measurements, it is essential to estimate its influence, either by calculation or by measurement, in order to subtract it from the measurement results.

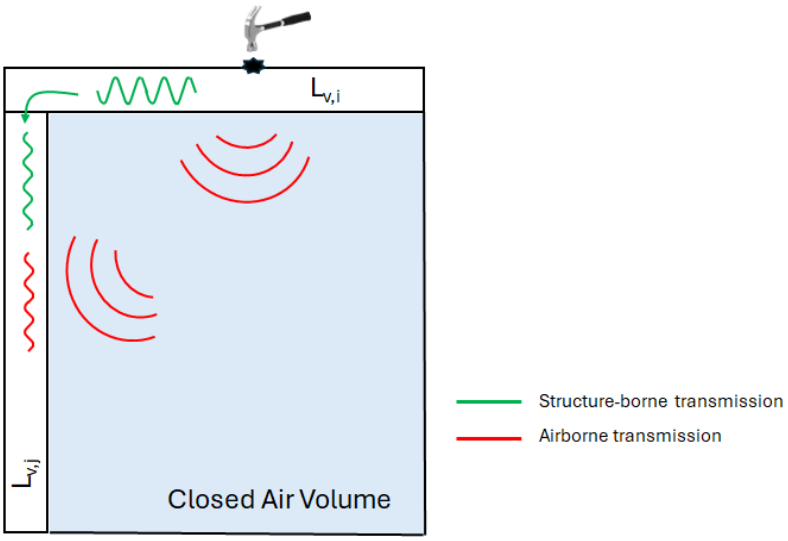

Figure 1 - Airborne and structure-borne transmissions which contribute to the vibration level of wall 'j' when wall 'i' is excited by mechanical excitation.

This article deals only with the problem of the contribution of parasitic airborne noise where the excited wall (transmitting wall) and the receiving wall are connected to a common volume of air through which airborne transmission occurs. In laboratories that build their mock-ups in closed cells, it concerns, for example, measurements between elements i and j in the situations shown in Figure 2.

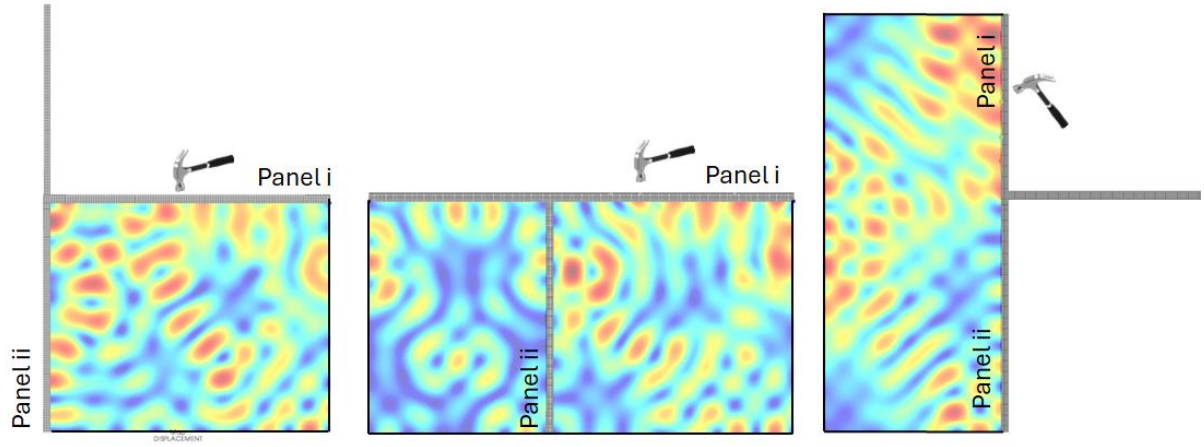

Figure 2 - Identification of the air volume responsible for parasitic airborne noise transmission between walls "i" and "j"

In laboratories that set up their mock-ups in large halls, all the walls are exposed to the same volume of air and the airborne contribution will depend on the volume of the hall, its reverberation and the direct or indirect exposure of the receiving wall to the radiation from the transmitting wall.

In the following, the significant contribution of airborne noise radiated by the transmitting panel on the vibration levels of the receiving panel is highlighted using a finite element model (FEM) and experimental results.

3. Finite Element Method analysis

The analysis of the contribution of airborne transmission, using finite element models (FEM), is carried out for a simple, idealised horizontal L-junction composed of two CLT panels with and without resilient strip. In this numerical simulation, the airborne noise produced in the closed air volume comes solely from the panel's acoustic radiation. Noise radiated by the impact of excitation source (such as hammer or tapping machine) on the panel is neglected. In the simulation, it is considered only the air volume between the two panels and not the outside air volume. Five configurations are modelled (fig.3) to determine the vibration reduction index including or disregarding the contribution of airborne noise radiated by the emitting wall through a closed air volume.

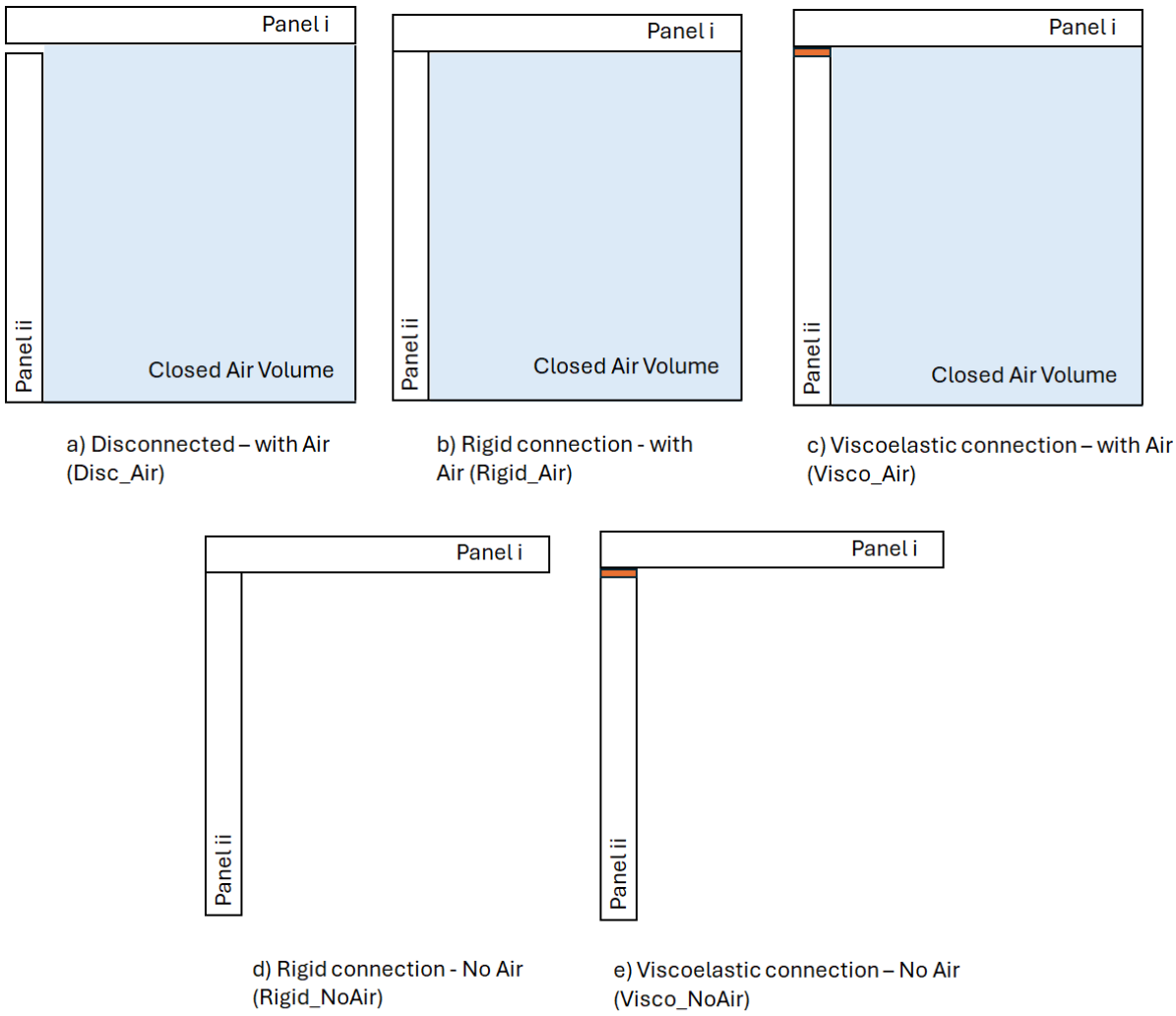

Figure 3 - The five configurations modelled with FEM

For the FEM calculations, the commercial software Actran (Version 15.1) [i] is used. To limit the computational cost, a 2D model is adopted, which is sufficient to get some initial insights. Panel i has a length of 4.9 m and a thickness of 14 cm. Panel ii has a length of 3.9 m and a thickness of 12 cm. The mesh size is 2 cm for the air volume and the CLT panels, and 1 mm in the thickness of the resilient strip. The CLT panels are modelled as isotropic solid materials and are characterised by the density ρ, Young's modulus E, Poisson's ratio μ and loss factor η (Table 1). The properties chosen for the CLT panels are those of the panels used in mock-up 2 (see section 4). The Young's moduli are the average Young's moduli measured in both directions using the longitudinal wave time-of-flight technique [22]. The loss factor is an adjusted trendline on values measured on the rigid configuration (direct contact between the CLT panels). The closed fluid volume is filled with air characterised by the density (ρ_0 = 1.2 kg/m³), speed of sound speed (ρ_0 = 340 m/s) and damping factor ($\eta = 2/f$). Simply supported boundary conditions are imposed on the free ends of the panels by restraining the transverse translational degree of freedom. The frequency range covered by the calculations are one-third octave bands between 50 Hz and 5000 Hz. Calculations are performed at 25 frequencies per one-third octave band and averaged. Excitation on the source plate is applied using three non-correlated point forces. The source positions are chosen according to the criteria described in ISO 10848-1 for laboratory measurements of K_{ij}. Radiating surfaces are used to obtain the mean

square velocity of each panel which are used to calculate the velocity level differences $D_{v,ij}$, $D_{v,ji}$ and the K_{ij}.

Table 1 - Material properties used for the simulations

	Thickness [m]	Density [kg/m³]	Young's Modulus [N/m²]	Poisson's ration [-]	Loss factor [-]
Panel i (CLT 5-ply)	0.14	486	3.7e+9	0.2	(*)
Panel ii (CLT 5-ply)	0.12	471	4.05e+9	0.2	(*)
Resilient layer	0.005	200	2e+5	0.4	0.2

(*) a frequency dependent loss factor is used following the law: $\eta = 0.0174\exp(-0.000194f)$

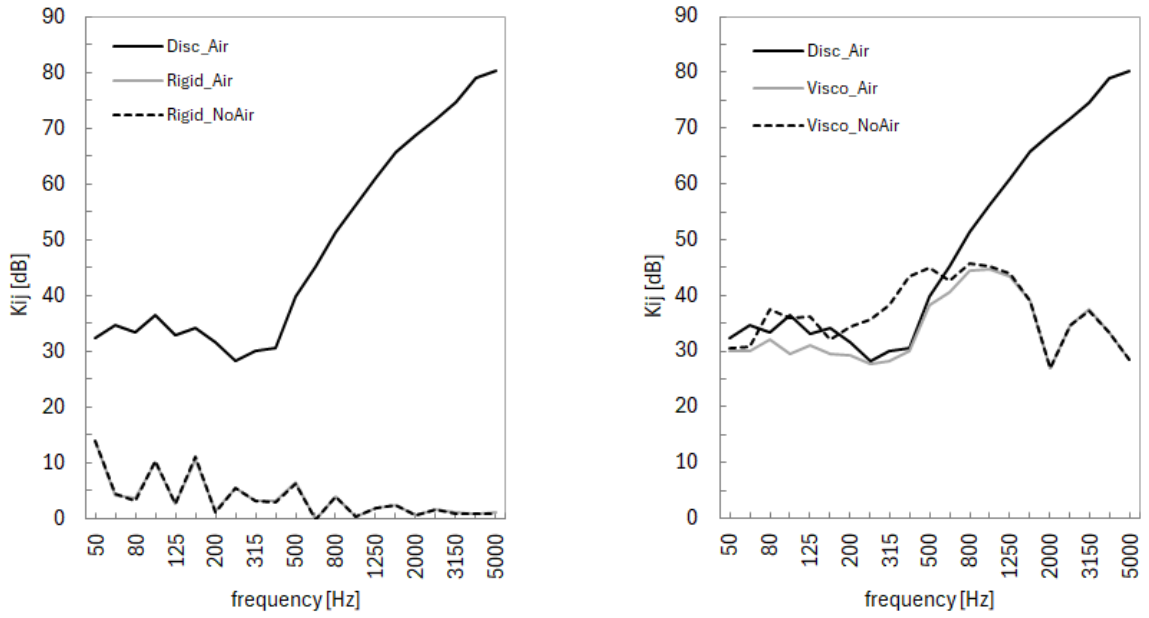

(a) (b)

Figure 4 - The FEM simulated K_{ij} for the cases where only airborne transmission is present (black line), structure borne and airborne transmissions are present (grey line) and where only structure-borne transmission is present (dashed line) for the rigid junction (a) and for the junction comprising a viscoelastic strip (b).

Figure 4a compares the K_{ij} of the rigid junction obtained in the case where there is either only a structure-borne transmission (Rigid_NoAir) or only an airborne transmission (Disc_Air) or both transmissions (Rigid_Air). The 'Rigid_NoAir' and 'Rigid_Air' curves do not show any significant differences and, therefore, clearly reveal that structure-borne transmission is not influenced by airborne transmission: structural transmission is dominant. Taking the analysis a little further, it can be observed that the presence of airborne transmission causes a maximum underestimation of 0.5 dB at 160 Hz in the assessment of the attenuation of structure-borne transmission occurring at this L-junction.

Figure 4b shows that the K_{ij} obtained for configuration "Visco_Air", for which the structure-borne and airborne transmission are present, is strongly conditioned by the airborne transmission below 500 Hz and by the structure-borne transmission above this frequency. Around 315 Hz, the presence of airborne transmission causes an underestimation of 8 dB in the assessment of the attenuation of structure-borne transmission occurring at this L-junction comprising a resilient strip.

The sharp decay observed at 2000 Hz for the cases with viscoelastic connection is caused by the first thickness resonance in the viscoelastic layer. An approximate value of this resonance frequency is given by [23]:

$$f_1 = \frac{1}{4h}\sqrt{\frac{E(1-\mu)}{(1+\mu)(1-2\mu)}\frac{1}{\rho}} \tag{3}$$

where h is the thickness, μ the Poisson's ratio, E the Young's modulus and ρ the density of the viscoelastic material. By determining this thickness resonance frequency from measurement results, the Young's modulus of the viscoelastic material under its operational load can be determined.

4. Measurement set-up and results

4.1. Mock-ups

Two full-scale mock-ups of CLT junctions were realised to measure the vibration reduction index.

The first CLT mock-up (mock-up 1, fig.5) realised at the University of Bologna in Italy, is a horizontal T-junction with floor dimensions of 360x240 cm^2 and wall dimensions of 300x240 cm^2, both 5-ply 10 cm thick. The top wall (panel iv) was fixed to the floor (panel i) by two small angle brackets. The floor (panel i) rests on one side on panel ii and on the other on wooden beams isolated from the heavy foundation slab by viscoelastic materials, thus preventing any structural transmission via the laboratory structure. The big black angle brackets visible in the picture between panels i and ii are needed for safety reasons but do not touch panel ii and are only attached to panel i.

Only the transmission between panel i and panel ii is studied in this paper. The accelerometers for measuring the velocity level were attached via magnets to screws in the panels, the excitation sources were vibro-transducers. The signal used for measuring velocity level was pink noise, and the signal used for measuring the structural reverberation time was MLS. Mock-up 1 was located inside the laboratory warehouse where the panels are entirely subject to parasitic noise.

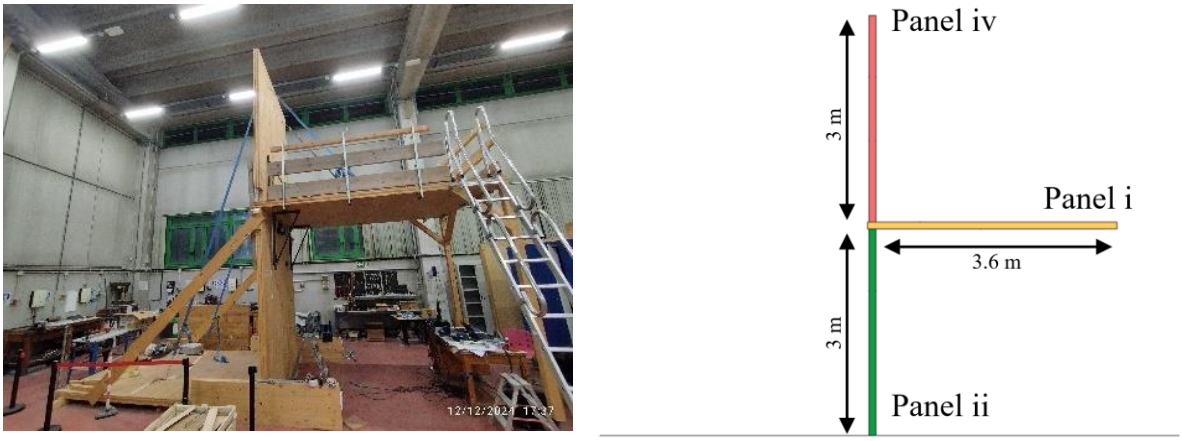

Figure 5 - Mock-up 1 of the University of Bologna (Italy)

The second CLT mock-up (mock-up 2, fig.6), realised in Belgium at Buildwise, was a horizontal L-junction with a floor dimension of 493x225 cm², 5-ply, 14 cm thick and a wall dimension of 394x240 cm², 5-ply, 12 cm thick. Panel ii was placed vertically between two acoustic cells (named E and F), but without any structural contact with them except at the foundation of acoustic cell E, which is decoupled from cell F. It protrudes 60 cm above the cells. The horizontal panel i was placed on one side on panel ii and on the other side on concrete blocks resting on the ceiling of cell F. In this configuration, energy transfer between panels i and ii can only take place structurally via the junction or by airborne transmission, the latter being limited, however, since only the small 60 cm portion of panel ii protruding from the cells can pick up or radiate airborne noise. To ensure maximum contact between the floor and the wall, a very thin layer of mortar was used to rectify the slight roughness and non-flatness of the wood. Glued accelerometers were used to measure the velocity level of the panels, and the excitation source was a hammer. In order to evaluate the effects of parasitic airborne noise in the K_{ij} measurement, several configurations were realised in which the amount of parasitic airborne noise transmission is changed.

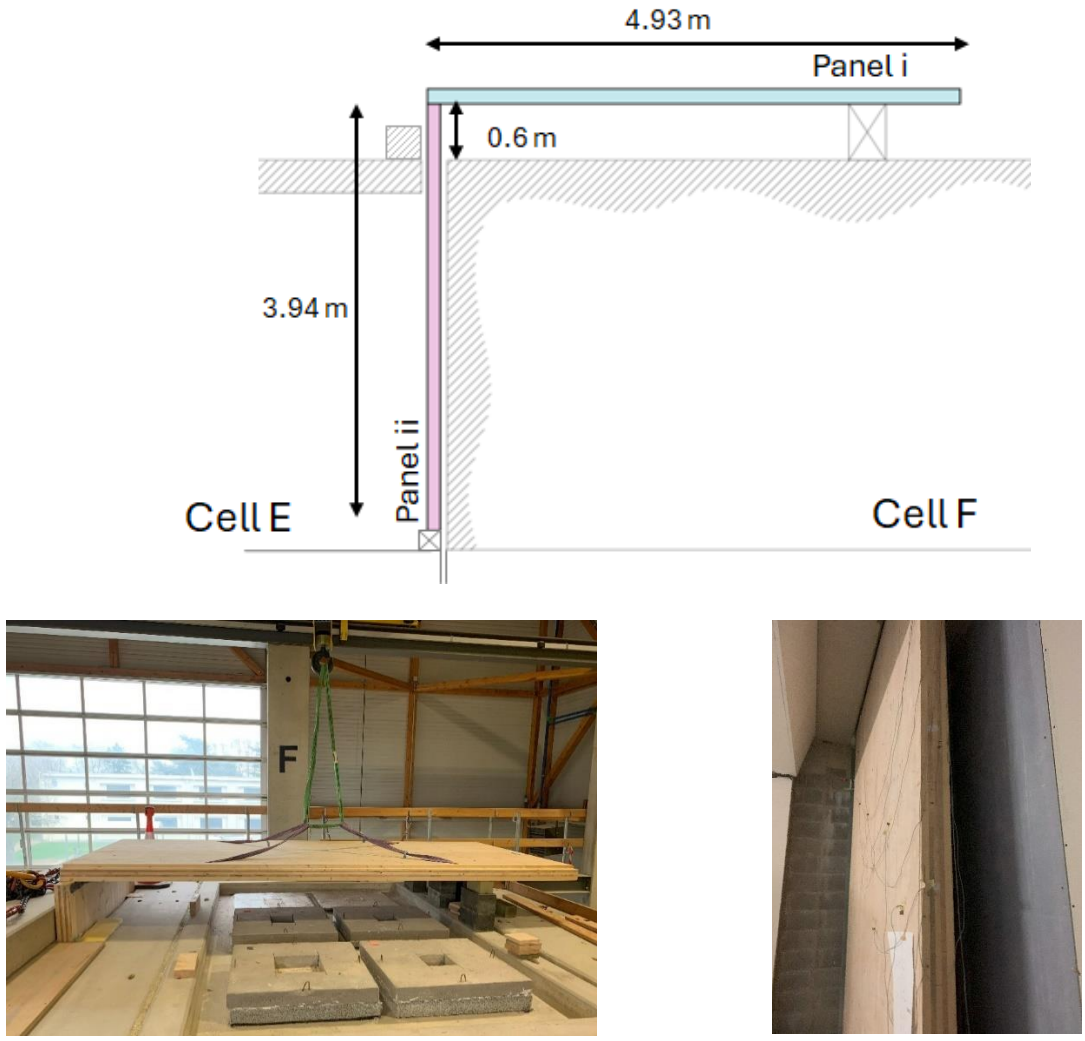

Figure 6 - Mock-up 2 of Buildwise (Belgium)

The positions of measuring points and source points in both mock-ups are compliant with ISO 10848-1.

It's important to note here that the airborne noise in both mock-ups comes from the radiation from the panels, but also from the noise generated by the exciter sources themselves: the vibro-transducers for mock-up 1 and the hammer for mock-up 2. However, it can be assumed that this noise is negligible compared to the noise radiated by the excited panel. Furthermore, the air volumes are not closed volumes but open volumes.

4.2. Tested configurations

The originality of the mock-ups is that it was possible to carry out measurements with the two panels completely decoupled and thus measure the panel vibration levels generated solely by parasitic airborne noise (Table 2). For mock-up 1 (1_conf.0), this was made possible by raising and supporting the floor (panel i) on two shoring props at a slightly higher height than the wall (panel ii) and, for mock-up 2 by holding the floor (panel i) raised using an overhead crane. In this mock-up, where only a limited part of panel ii is exposed to airborne noise (60 cm), two different configurations were tested: one without a lining (2_conf.0a) and the other with a lining covering both sides of the small part of panel ii exposed to airborne noise (2_conf.0b).

In this latter configuration, the influence of parasitic airborne noise is considerably reduced. Indeed, as a receiver, panel ii is protected from airborne noise emitted by panel i. Conversely, when panel ii is the source panel, the lining limits the radiation of airborne noise towards the receiving panel i.

Table 2 – The tested junctions with decoupled panels

Mockup	Configuration	Junction contact	Linings	Scheme
1	1_conf.0	decoupled	no	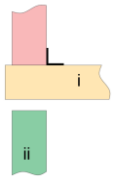
2	2_conf.0a	decoupled	no	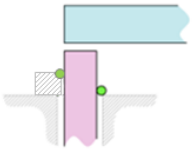
2	2_conf.0b	decoupled	yes	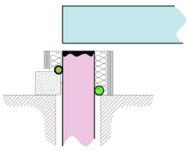

Measuring the $\overline{D_{v,ij}}$ in the configurations "1_conf.0", "2_conf.0a" and "2_conf.0b" and normalising this value with respect to the length of the junction (the length of the hypothetical junction if there had been contact) gives an estimate of the maximum K_{ij}, named $K_{ij,\max,}$ that can be measured in these mock-ups.

Afterwards, several configurations with rigid junctions (direct contact between CLT panels) and junctions with resilient strips were tested. Table 3 shows the three rigid configurations that were tested in both mock-ups. Table 4 shows the different configurations tested with a resilient strip. The resilient material used is the same expanded EPDM product in strip form of 6mm thickness for both the mock-ups, in particular for mock-up 1 the width is 10mm for the entire length of the junction (2.4m) while for mock-up 2 the width is 8mm for the entire length of the junction (2.25m). All measurements with resilient material are made without pre-loading time, i.e. less than 10 minutes from being placed under the structure's own weight and being measured. For mock-up 1, the load equals half the weight of the floor (panel i) plus the weight of the upper panel (panel iv) [pressure of 0.024 N/mm^2 on the resilient material] and, for mock-up 2, the load (without concrete blocks) equals half the weight of the floor (panel i) [pressure of 0.021 N/mm^2 on the resilient material].

Table 3 - The tested rigid junctions

Mock-up	Configuration	Junction contact	Linings	Scheme

1	1_conf.1	rigid junction*	no	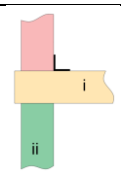
2	2_conf.1a	rigid junction with thin layer of mortar to ensure perfect contact	no	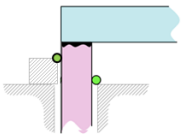
2	2_conf.1b	rigid junction with thin layer of mortar to ensure perfect contact	yes	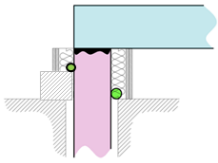

* the upper angle bracket is for safety reasons and does not connect panels i and ii.

Table 4- The junctions with resilient strips tested

Mock-up	Configuration	Junction contact	Linings	Scheme
1	1_conf.2	resilient strip (pressure of 0.024 N/mm²)	no	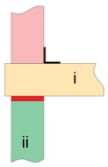
1	1_conf.3	resilient strip + 6 screws (pressure of 0.024 N/mm²)	no	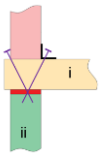
2	2_conf.2a	resilient strip (pressure of 0.021 N/mm²)	no	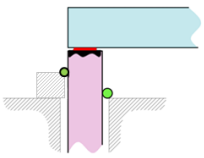
2	2_conf.2b	resilient strip (pressure of 0.021 N/mm²)	yes	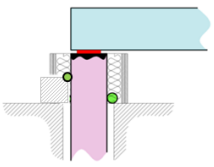
2	2_conf.3	Junction with a resilient + a load of 3 concrete blocks (pressure of 0.079 N/mm²)	no	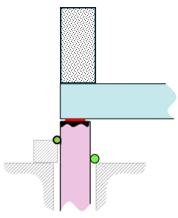

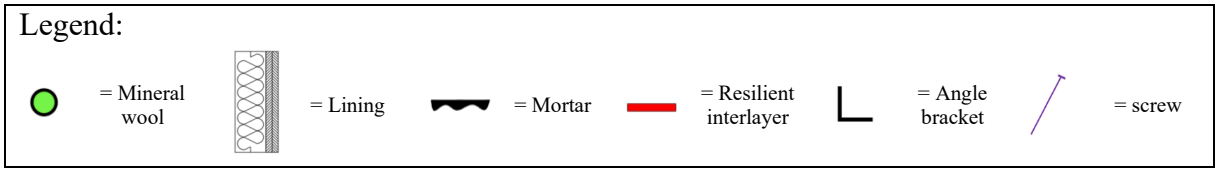

Figure 7 compares the $K_{ij,\max}$ measured in the two mock-ups. They differ only beyond the critical frequency of the CLT panels, which is around 165 Hz for the panel i of the mock-up 2, 181 Hz for the panel ii of the mock-up 2 and 227 Hz for the panels of the mock-up 1. As expected, mock-up 1 (1_conf.0) has the lowest $K_{ij,max}$ because, on the one hand, the properties of the panels favour a greater contribution from airborne noise (higher critical frequency and lower mass per unit area of the panels in mock-up 1 compared with mock-up 2) and, on the other hand, the total surfaces of the panels can be excited by or radiate airborne noise. Mock-up 2 with linings (2_conf.0b) has the highest $K_{ij,\max}$. However, at 250 Hz mock-up 2 (2_conf.0a and 2_conf.0b) has a lower $K_{ij,\max}$ than mock-up 1 (1_conf.0). This can be explained by the fact that at this frequency, where the radiation efficiency of the CLT panels is at its maximum, a modal effect is added due to the air cavity under the floor in mock-up 2. It should also be noted that the lining, which is poorly dimensioned, aggravates the situation due to its 'mass-spring' effect at this frequency and gives no improvement below 250 Hz.

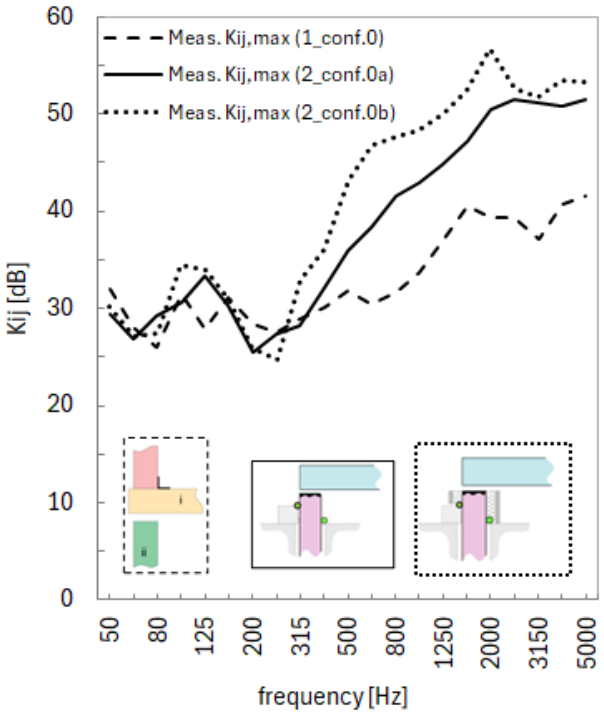

Figure 7 - Comparison of $K_{ij,\max}$ measured in mockup 1 and mockup 2

4.3. Influence of airborne noise for the rigid junctions

With the measurements of $K_{ij,\max}$, it is possible to check whether the airborne transmission is negligible compared with the structural transmission and whether a correction needs to be

applied to the measured vibration reduction indices $K_{ij,\mathrm{meas}}$. If the difference between $K_{ij,\mathrm{max}}$ and $K_{ij,\mathrm{meas}}$ is greater than or equal to 4 dB, the result of the measurement is corrected for the influence of the airborne transmission in any of the frequency bands by calculating $K_{ij,\mathrm{corrected}}$ as given by:

$$K_{ij,\mathrm{corrected}} = -10\lg\left(10^{-K_{ij,\mathrm{meas}}/10} - 10^{-K_{ij,\mathrm{max}}/10}\right) \quad (4)$$

If the difference ($K_{ij,\mathrm{max}}$ - $K_{ij,\mathrm{meas}}$) is larger than 15 dB, the correction is negligible and $K_{ij,\mathrm{corrected}}$ equals $K_{ij,\mathrm{meas}}$. If the difference ($K_{ij,\mathrm{max}}$ - $K_{ij,\mathrm{meas}}$) is less than 4 dB, it is impossible to eliminate the airborne noise contribution due to the reproducibility limits of the measurement. In this case, a maximum correction of 2.2 dB is applied:

$$K_{ij,\mathrm{corrected}} = K_{ij,\mathrm{meas}} + 2.2 \text{ dB} \quad (5)$$

This correction corresponds to a difference of 4 dB. It's important to note that, in this case, $K_{ij,\mathrm{corrected}}$ will be a minimum value. The low limit of 4 dB for the application of the correction is made possible by a low measurement uncertainty in the mid-range frequencies.

Figure 8 shows the $K_{ij,\mathrm{max}}$, the measured K_{ij} and the K_{ij} corrected according to Eqs. (4) and (5) for the three rigid junction configurations. The shaded areas on the graphs indicate the measurement standard uncertainties. As the junction is rigid, structure-borne transmission is expected to dominate. This is confirmed by the measurement results. In mock-up 1 (fig.8a), the maximum contribution from airborne transmission occurs at 80 Hz resulting in a 0.6 dB underestimation of the measured value at this frequency. For configurations "2_conf.1a" and "2_conf.1b" of mock-up 2 (fig.8b and fig.8c), the maximum contribution from airborne transmission occurs around 200 Hz leading to a 0.5 dB and 1.1 dB underestimation of the measured values, respectively. In the case of these rigid junctions, the correction is smaller than the measurement uncertainty over the entire frequency range. However, a correction is desirable because the parasitic noise introduces a systematic underestimation of K_{ij}, which introduces a biased but non-random error. So even if the correction is less than the measurement uncertainty, it is still advisable to guarantee the accuracy of the measurement.

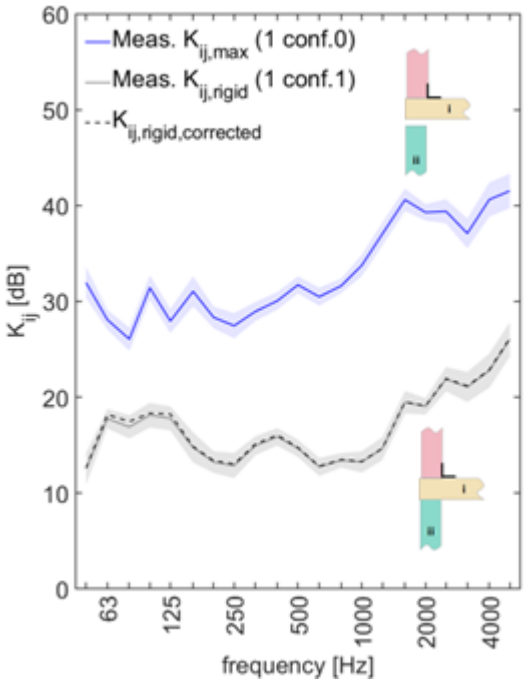
Meas. $K_{ij,max}$ (1 conf.0)
Meas. $K_{ij,rigid}$ (1 conf.1)
$K_{ij,rigid,corrected}$
K_{ij} [dB]
frequency [Hz]
0
10
20
30
40
50
60
63
125
250
500
1000
2000
4000

(a)

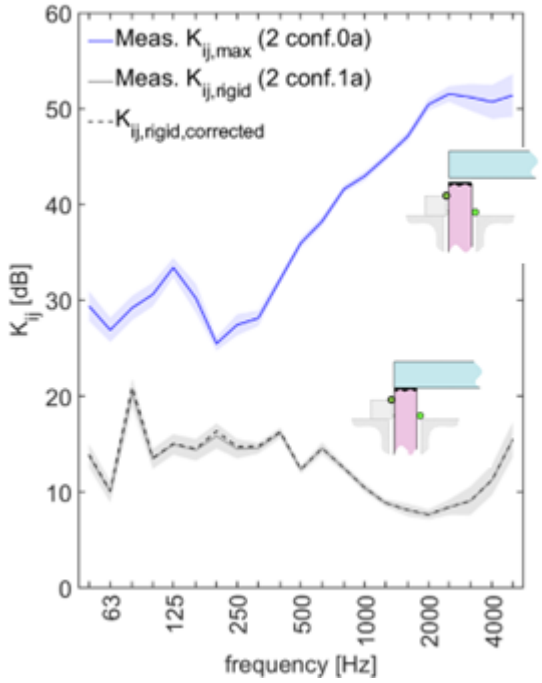
Meas. $K_{ij,max}$ (2 conf.0a)
Meas. $K_{ij,rigid}$ (2 conf.1a)
$K_{ij,rigid,corrected}$
K_{ij} [dB]
frequency [Hz]
0
10
20
30
40
50
60
63
125
250
500
1000
2000
4000

(b)

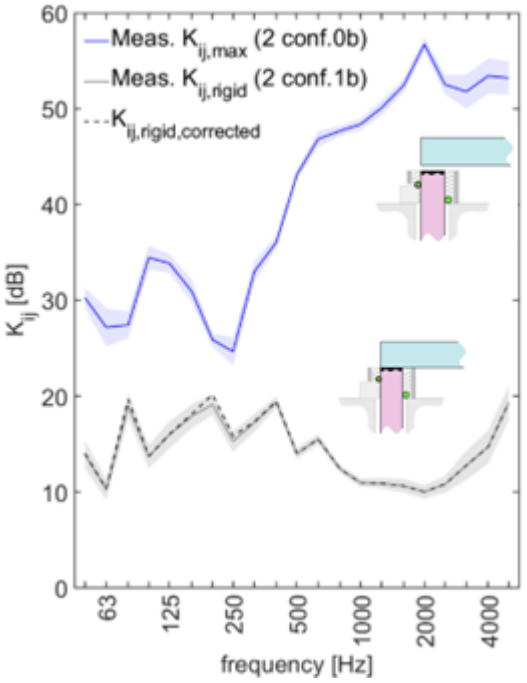
Meas. $K_{ij,max}$ (2 conf.0b)
Meas. $K_{ij,rigid}$ (2 conf.1b)
$K_{ij,rigid,corrected}$
K_{ij} [dB]
frequency [Hz]
0
10
20
30
40
50
60
63
125
250
500
1000
2000
4000

(c)

Figure 8– The measured (grey line) and corrected (dotted line) K_{ij} for the rigid junctions in (a) mock-up 1, (b) mock-up 2 and (c) mock-up 2 with lining. $K_{ij,max}$ (blue line) is also shown for comparison. The shaded areas indicate the standard uncertainty.

4.4. Influence of airborne noise for the junctions with a resilient strip

Applying a resilient strip at a junction considerably reduces structure-borne noise transmission. In the frequency range where the wavelengths are smaller than the dimensions of the panels the resilient strip provide a linear increase in K_{ij} as a function of frequency until the first thickness mode appears (see Eq. 3), where the K_{ij} drops drastically. Since the resilient strip considerably reduces structure-borne transmission, the relative contribution of airborne transmission to the total transmission will increase. The contribution of the airborne transmission can be seen in Figure 9.a where the difference ($K_{ij,max}$ - $K_{ij,meas}$) is less than 15 dB over the entire frequency range of interest (except at 50 Hz) and thus the correction according to Eq. (4) is not negligible. According to the measurements, the first thickness resonance is located at 3150 Hz. Around this frequency, i.e. between 2000 Hz and 5000 Hz, the influence of airborne transmission on the measured K_{ij} is negligible. For this configuration, the difference between corrected and uncorrected K_{ij} ($K_{ij,resilient,corrected}$ - $K_{ij,resilient}$) is statistically relevant ($p < 0.05$) between 200 Hz and 1000 Hz, which fully justifies the application of corrections over this frequency range. Outside this frequency range, the correction is still recommended to improve the accuracy of the results by compensating for the systematic error.

When screws pierce the resilient strip (fig.9b), the structure-borne transmission increases, and the contribution of the airborne transmission is reduced. The first thickness resonance is still weakly noticeable. On average, between 200 Hz and 1250 Hz, the K_{ij} is underestimated by 0.5 dB by the measurement when no correction is made for the airborne transmission.

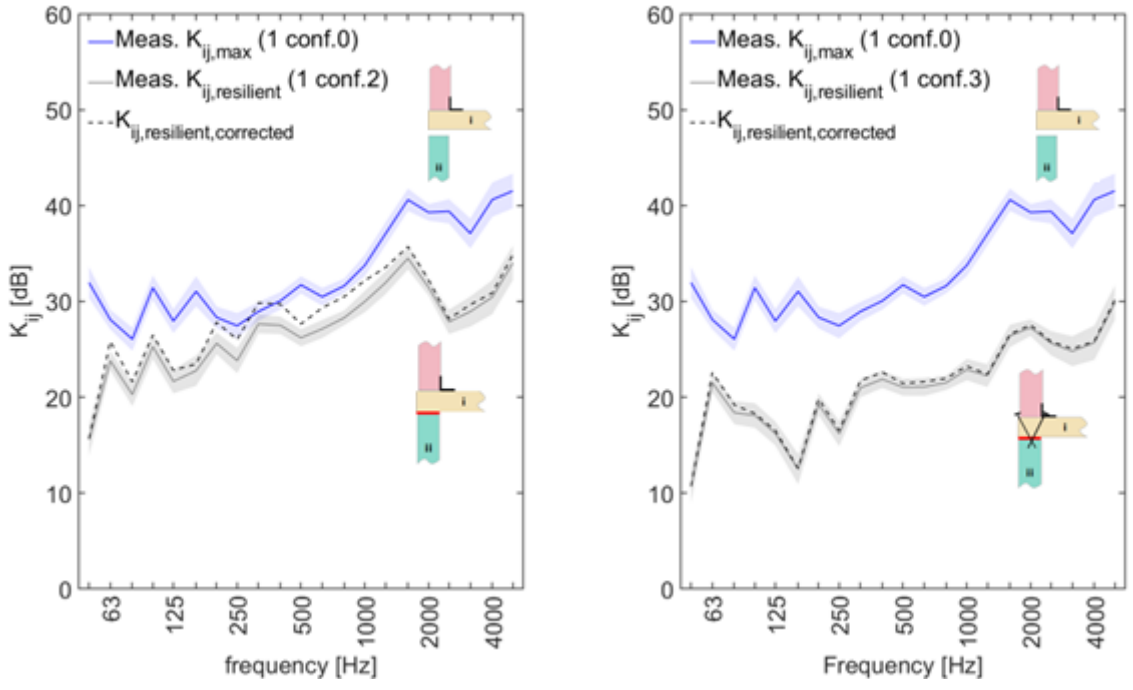

(a) (b)

Figure 9 - The measured (grey line) and corrected (dotted line) K_{ij} for the junctions with resilient strip in mock-up 1 (a) without and (b) with screws. $K_{ij,\max}$ (blue line) is also shown for comparison. The shaded areas indicate the standard uncertainty.

For mock-up 2 (fig.10a), the difference ($K_{ij,\max}$ - $K_{ij,\text{meas}}$) is less than 15 dB over the frequency range between 50 and 1600 Hz. The maximum correction of 2.2 dB is applied between 200 Hz and 400 Hz where the airborne contribution is largest. Between 500 Hz and 1250 Hz, the average correction is 1.2 dB. As for 1_conf.2, the difference between the corrected and uncorrected K_{ij} values ($K_{ij,resilient,corrected}$ - $K_{ij,resilient}$) is statistically significant in the 200 Hz to 1000 Hz range.

In the configuration where the resilient strip is more compressed (fig.10b), its efficiency reduces, and the contribution of the airborne transmission also reduces. A maximum correction of 2.2 dB is still applied between 200 Hz and 400 Hz, but the correction reduces to 0.6 dB between 500 Hz and 1250 Hz. Compressing the resilient strip shifts the thickness resonance frequency from 2500 Hz to 3150 Hz.

For the configuration with linings (fig.10c) the influence of airborne noise is limited to a narrower range of frequencies, from 160 Hz to 500 Hz instead of 160 Hz to 1600 Hz for the configuration without linings. The linings therefore thus proved efficient in limiting the airborne noise between 500 Hz and 1600 Hz. However, around 250 Hz, airborne noise is still affecting the measurement because of the mass-spring effect of the lining in this frequency range.

As expected, for these last two configurations, the correction is statistically relevant only in the 200 Hz to 400 Hz range.

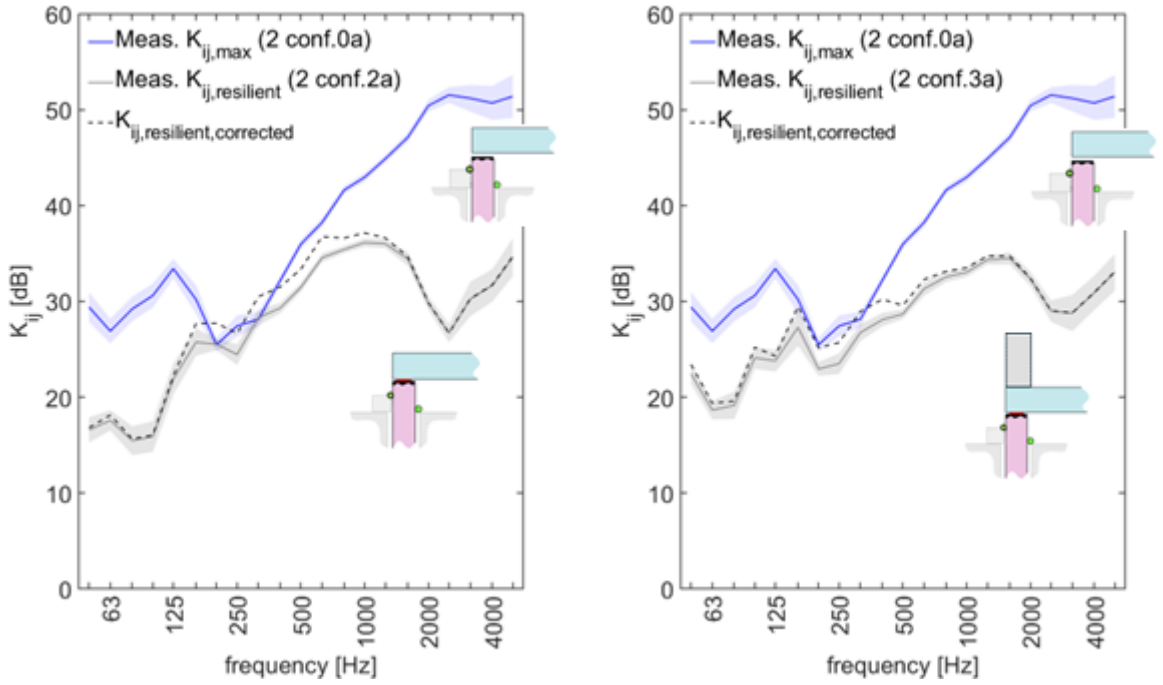

(a)

(b)

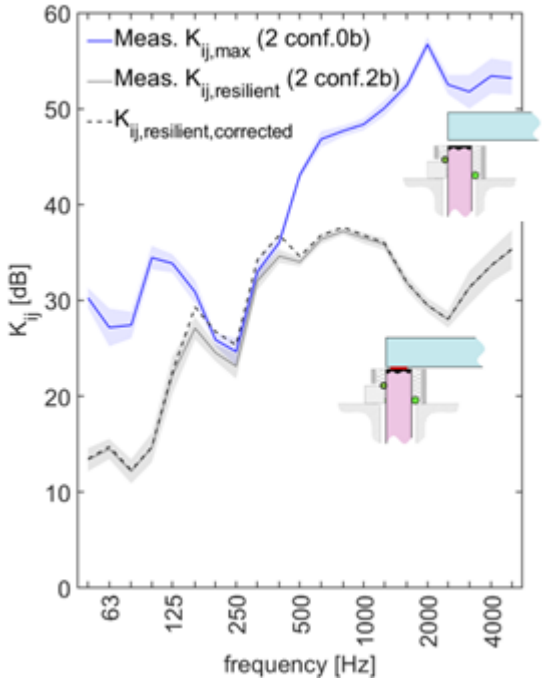

(c)

Figure 10 - The measured (grey line) and corrected (dotted line) K_{ij} for the junctions with resilient strip in mock-up 2 (a) without linings and without loading, (b) without linings and with loading and (c) with linings and without loading. $K_{ij,max}$ (blue line) is also shown for comparison. The shaded areas indicate the standard uncertainty.

5. Implications for predictive calculations

The measured K_{ij}-values can be used to compare the performance of different junctions and also as input data for predictive calculations following the ISO 12354 standards series. An underestimation of the K_{ij}-values obtained during a measurement influenced by parasitic airborne noise therefore leads to an underestimation of the acoustic performance between rooms. To illustrate this effect, predictive calculations of airborne sound insulation between two superimposed rooms of 45 m³, made of 10 cm thick CLT panels (mock-up 1), were carried out in accordance with the standard ISO 12354-1. In this example, shown in Figure 11, it is assumed that the four junctions between the flanking walls of the upper room (denoted F1, F2, F3 and F4) and the floor (denoted d) incorporate a screwless resilient strip, corresponding to configuration 1_conf.2 in Figure 10.a. The predictive calculation indicates that the $D_{nT,w,F\text{-}d}$, determined only from the transmission paths F1d, F2d, F3d and F4d and based on the K_{ij} influenced by the parasitic airborne noise, is 1 dB lower than the predictive result obtained with the corrected K_{ij}.

It is important to note that, if K_{ij} is clearly defined as an indicator of performance in terms of structure-borne transmission, the question arises as to the extent to which parasitic airborne transmission between elements should be included in the predictive calculations of the ISO 12354 standards series.

The predicted values of $D_{n,f}$ or $D_{nT,f}$ should reflect reality as closely as possible. Thus, if the elements of the high-performance junction are fitted with a lining or a floating screed, the corrected K_{ij} must be used for the predictive calculations. In the illustration (fig.11), the floor is fitted with a floating screed, so it is protected from parasitic airborne noise. The predictive calculation must therefore take into account the corrected K_{ij}. If no lining or floating screed is present, parasitic airborne transmission must be taken into account. It remains to be determined how to integrate this parasitic transmission, since it depends on the properties of the building elements, the volume of the room and its reverberation time.

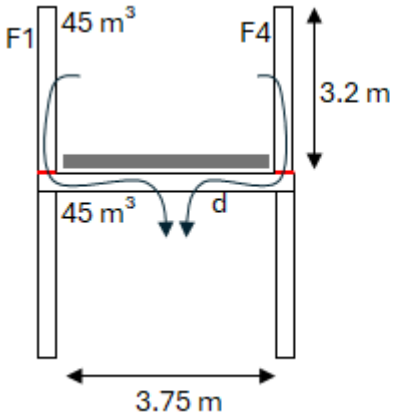

If K_{ij} of the F-d path* is **not corrected** and is influenced by parasitic airborne noise :
$D_{nTw,F\text{-}d}$=**56** (-1;-5)dB

If K_{ij} of the F-d path* is **corrected** so that it is not influenced by parasitic airborne noise:
$D_{nTw,F\text{-}d}$=**57** (-1;-4)dB

* F-d path = F_1-d+F_2-d+F_3-d+F_4-d paths

Figure 11– Calculation of the standardized flanking level difference for the F-d path in a CLT mock-up with and without Kij correction.

6. Conclusion

The article deals with certain considerations to be taken into account when measuring the vibration reduction index K_{ij} or the normalized direction-average vibration level difference, $\overline{D_{v,ij,n}}$ in the laboratory in accordance with the ISO 10848-1 standard. During measurement, in addition to structural transmission through the junction of the panels, there is also parasitic airborne transmission which can influence the results. This unwanted airborne noise comes from the acoustic radiation of the excited panel and the noise generated by the source itself, which excites the receiving panel and leads to an underestimation of K_{ij}. In tests carried out on laboratory mock-ups without lining, this airborne contribution can have a significant impact, particularly for high-performance junctions, such as those incorporating a resilient strip. When it comes to comparing the effectiveness of different systems for reducing structure-borne transmissions at junctions, or to obtain reliable data for predictive models, it is essential to implement specific measures to assess and/or eliminate these parasitic airborne transmissions.

Numerical simulations using the finite element method, together with measurements carried out on two CLT models in two laboratories have highlighted the influence of parasitic airborne noise on the K_{ij} measurements. The paper shows that a correction based on the subtraction of the $K_{ij,\max}$ - measured on a fully decoupled junction - can be applied to obtain more accurate results.

An example shows that the standardized flanking level difference between CLT rooms, for the path F-d comprising a resilient strip, can be underestimated by 1 dB if the K_{ij} is not corrected for a case where the floor is fitted with a floating screed. However, when the elements of a junction incorporating a resilient strip are not equipped with a lining or floating screed, it may be appropriate to consider the influence of parasitic air transmission in the predictive calculations of the ISO 12354 standards, as well as how to incorporate it.

Wherever possible, it is therefore recommended that laboratories carry out a specific measurement of the $K_{ij,\max}$ for their mock-up. However, such a measurement may prove difficult, or even impractical, in many situations. To limit the influence of airborne noise during tests, it may therefore be necessary to implement practical solutions in the experimental set-up. One effective approach is to fill the air volumes common to the walls under test with porous and fibrous materials. This method avoids the use of lining, which could be incompatible with the installation of accelerometers and lead to an undesirable mass-spring-mass effect. In addition, it is recommended to apply acoustic protection to noisy excitation systems, such as tapping machines.

Acknowledgements
Charlotte Crispin and Arne Dijckmans are grateful for the financial support from the Federal Public Service Economy of Belgium. The authors are grateful to Jonathan Jacqmot from Quiet Consult for his expert advice on the numerical simulations.

References

[1] ISO 12354-1, "Building acoustics - Estimation of acoustic performance of buildings from the performance of elements - Part 1: Airborne sound insulation between rooms," in *European Standard*, 2017.

[2] ISO 12354-2, "Building acoustics - Estimation of acoustic performance of buildings from the performance of elements - Part 2: Impact sound insulation between rooms," 2017.

[3] E. Gerrestsen, "Calculation of airborne and impact sound insulation between dwellings," *Applied Acoustics 19,* pp. 245-264, 1986.

[4] ISO 10848-1, "Acoustics - Laboratory and field measurement of flanking transmission for airborne, impact and building service equipment sound between adjoining rooms - Part 1: Frame document," 2017.

[5] A. Osipov and G. Vermeir, "Sound transmission in buildings with elastic layers at joints," *Applied Acoustics 49,* pp. 143-162, 1996.

[6] R. Craik and A. Osipov, "Structural isolation of wall using elastic interlayers," *Applied Acoustics 46,* pp. 233-249, 1995.

[7] D. B. Pedersen, "Estimation of vibration attenuation through junctions of building structures," *Applied Acoustics 46,* pp. 285-305, 1995.

[8] P. Mees and G. Vermeir, "Structure-borne sound transmission at elastically connected plates," *Journal of sound and vibration 166,* pp. 55-76, 1993.

[9] C. Crispin, B. Ingelaere and G. Vermeir, "Innovative building systems to improve the acoustical quality in lightweight masonry constructions: Application of resilient joints at junctions - PART 1: analysis of the experimental results," in *Euronoise*, Paris, 2008.

[10] M. Schneider and H.-M. Fisher, "Flanking transmission of masonry building elements with flexible interlayer," in *Forum Acusticum*, Budapest, 2005.

[11] A. Dijckmans, V. Possenti Pettoni, L. Barbaresi and C. Crispin, "Vibration reduction index improvement by adding resilient strips: influence of junction properties," in *Inter-Noise*, Nantes, 2024.

[12] L. Barbaresi, A. Di Bella, V. Pettoni Possenti, M. Salvalaggio and M. Rosa Valluzzi, "Comparative analysis of vibroacoustic measurements in a CLT building mock-up," in *International congress on acoustics*, Gyeongju, 2022.

[13] P. Brugnara, A. Speranza, L. Barbaresi, V. Pettoni Possenti and L. Sestigiani, “On the laboratory study of junction in flanking transmission in timber buildings,” in *Forum Acusticum*, Torino, 2023.

[14] S. Schoenwald, N. Kumer, S. Wiederin, N. Bleicher and B. Furrer, “Application of elastic interlayers at junctions in massive timber buildings,” in *International Congress on acoustics*, Aachen, 2019.

[15] S. Moons, R. Lanoye and E. Reynders, “Prediction of flanking sound transmission through cross-laminated timber junctions with resilient interlayers,” *Applied Acoustics 228,* 2025.

[16] C. Crispin and A. Dijckmans, “A standardized measurement method to measure the vibration reduction index improvement by adding resilient strips at a wall-floor junction: preliminary exercise,” in *Inter-Noise*, Seoul, 2020.

[17] A. Santoni, S. Schoenwald, P. Fausti and H.-M. Tröbs, “Modelling the radiation efficiency of orthotropic cross-laminated timber plates with simply-supported boundaries,” *Applied Acoustics 143,* pp. 112-124, 2019.

[18] F. Morandi, A. Prato, L. Barbaresi and A. Schiavi, “On the diffuseness of the vibrational field of a cross-laminated timber plate: Comparison between theoretical and experimental methods,” *Applied Acoustics,* p. vol 159, 2020.

[19] A. Di Bella and M. Mitrovic, “Acoustic Characteristics of Cross-Laminated Timber Systems,” *MDPI,* p. Vol 12, 2020.

[20] J. Mahn and M. Müller-Trapet, “Characterization of laminated timber building elements to estimate flanking transmission,” in *Inter-Noise*, Madrid, 2019.

[21] S. Vallely and S. Schoenwald, “Higher-order modal parameter estimation and verification of cross-laminated timber plates for structural-acoustic analyses,” *Acta Acustica,* p. Vol 8, 2024.

[22] C. Hopkins, Sound Insulation, Burlington: Butterworth-Heinemann, 2007.

[23] M. Etchessahar, “Caractérisation mécanique en basses fréquences des matériaux acoustiques,” Ecole doctorale de l'Université du Maine, Le Mans, 2002.

[24] E. Gerretsen, “Calculation of the sound transmission between dwellings by partitions and flanking structures,” *Applied Acoustics,* 1979.

[25] E. Gerretsen, “European developments in prediction models for building acoustics,” *Acta Acustica 2,* pp. 205-214, 1994.

[26] C. Hopkins, “Measurement of the vibration reduction index, Kij on free-standing masonry wall constructions,” *Journal of Building Acoustics 6,* pp. 235-257, 1999.

[27] C. Crispin, B. Ingelaere and D. Wuyts, “Innovative building systems to improve the acoustical quality in lightweight masonry constructions: Application of resilient joints at

junctions - PART 2: Study cases modelled according to the standard 12354-1 (2000),” in *Euronoise*, Paris, 2008.

[28] R. Craik, Sound transmission trough buildings using statistical energy analysis, Hampshire: Ashgate, 1996.

[29] E. Nilsson, S. Ménard, D. Bard and K. G. Hagberg, “Effects of Building Height on the Sound Transmission in Cross-Laminated Timber Buildings—Vibration Reduction Index,” *Buildings 13,* 2023.

[30] S. Mecking, T. Kruse and U. Schanda, “Measurement and calculation of sound transmission across junctions of solid timber building elements,” in *EuroNoise*, Maastricht, 2015.

[31] F. Morandi, S. De Cesaris, M. Garai and L. Barbaresi, “Measurement of flanking transmission for the characterisation and classification of cross laminated timber junctions,” *Applied Acoustics 141,* pp. 213-222, 2018.

[i] Anon. Actran 15.1 User’s Guide. MSC Software Company (Free Field Technologies SA), April 2015.